Structural characterization, DNA binding study, antioxidant potential and antitumor activity of diorganotin(IV) complexes against human breast cancer cell line MDA-MB-231

Shaista Ramzan [a,b], Shaukat Shujah [a*], Katherine. B. Holt [b], Zia-ur-Rehman [c], Syed Tasleem Hussain [a], Jeremy Karl Cockcroft [b], Naila Malkani [d], Niaz Muhammad [e], Aneela Kauser [a]

[a] Department of Chemistry, Kohat University of Science and Technology, Kohat 26000, Pakistan

[b]Department of Chemistry, Christopher Ingold Laboratory, University College London WC1H0AJ UK,

[c]Department of Chemistry, Quaid-i-Azam University, Islamabad 45320, Pakistan

[d] Department of Zoology, Government College University, Lahore, Pakistan

[e]Department of Chemistry, Abdul Wali Khan University, Mardan, Pakistan

*Corresponding author:

Department of Chemistry, Kohat University of Science and Technology, Kohat 26000, Pakistan.

E–mail address: shaukat.shujah@yahoo.com (Shaukat Shujah)

Abstract

Five new organotin(IV) complexes, Me_2SnL (**1**), Bu_2SnL (**2**), t-Bu_2SnL (**3**), Ph_2SnL (**4**) and Oct_2SnL (**5**), have been synthesized from the reaction of R_2SnCl_2 (R= Me, Bu, *tert*-Bu, Ph, Oct) with N'-(3-ethoxy-2-hydroxybenzylidene)formohydrazide (**H_2L**). The structural elucidation of synthesized compounds was done by FT-IR, ^{1}H-NMR, ^{13}C-NMR spectroscopy and single-crystal X-ray analysis. Crystallographic data of complex (**1**) showed seven coordinated central tin atom with distorted pentagonal bipyramidal geometry. Where in solution the Sn atom of synthesized complexes exhibit five coordination, confirmed from ^{1}H-NMR. The results from DNA interaction studies via UV-visible spectroscopy, viscosity, cyclic voltammetry, and differential pulse voltammetry (DPV) suggested an intercalative mode of interaction between the synthesized compounds and SS-DNA. Furthermore, the complexes interact more significantly than ligand. Electrochemical and thermodynamic parameters, including diffusion coefficient, ΔH, ΔG, and ΔS, were calculated using cyclic voltammetry data. The linear plot of peak current (I) vs. square root of the scan rate ($\upsilon^{1/2}$) indicated the electrochemical processes to be diffusion controlled. The DPPH free radical scavenging assay results showed that complex (**4)** is an active antioxidant. *In-vitro* cytotoxicity of the synthesized compounds was determined on human breast cancer cell line MDA-MB-231 using tetrazolium-based MTT assay, and complexes (**2),** (**3)** and (**4)** showed significant cytotoxic activity. The structure-activity relationships may be utilised to direct the optimization of the activity of agents from this class of compounds by comparing the specifics of the compound structures, their DNA binding, and toxicity.

Keywords: Organotin(IV) complexes. Crystal structure. DNA-binding. Cyclic voltammetry. Cytotoxicity. DPPH antioxidant activity.

Graphical Abstract

DNA binding interaction of the new diorganotin(IV) complexes was studied by UV-Visible spectrophotometry, viscometry and electrochemical techniques. The antioxidant activity and cytotoxicity against human breast cancer cell line MDA-MB-231 was also determined.

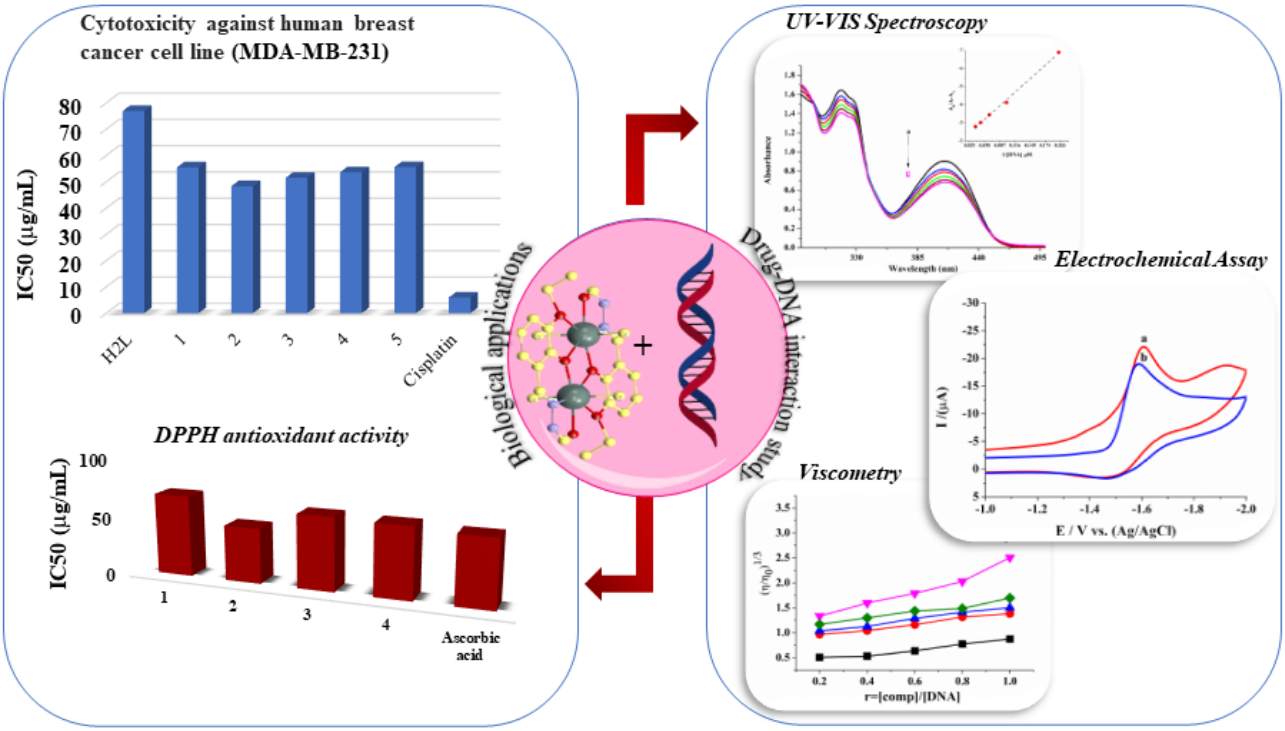

Introduction

The incidence and deaths due to cancer have gradually increased along with rising living standards. Chemotherapy, radiation, and surgery are currently the three main cancer treatments. Numerous platinum chemotherapy compounds, including carboplatin, oxaliplatin, nedaplatin, lobaplatin, and heptaplatin, have been researched and approved as anticancer medications [1], since the discovery of the first effective anticancer metallodrug cisplatin by Rosenberg in 1965 [2]. However, the adverse consequences of platinum-based chemotherapy [3-6] have prompted the development of non-platinum chemotherapeutics [7-11].

Organotin compounds have many applications including biological applications and are among the most commonly used organometallic compounds [12]. At a minimum, one direct covalent bond is present in organotin compounds between the organic group's central Sn atom and carbon atom (C). Recent research works reported the effect of organotin compounds on a range of human cancer cell lines [13-15], and Sn(IV) complexes of a wide variety of ligands [16-18] have shown anticancer activities mostly stronger than cisplatin against certain types of cancer [19, 20]. Organotin compounds also show good antiviral, antimicrobial [21], and anti-inflammatory activities [22]. The medicinal properties of organotin(IV) complexes are due to their unique molecular geometry, accessibility of coordination position around central tin atom, and ease of hydrolysis of ligands [23]. The inherent apoptotic inducing ability of these compounds makes them potential candidates for cancer treatment. Like other chemotherapy drugs organotins also exhibit cytotoxicity, however, the cytotoxicity can be modulated by changing the ligands or groups at equatorial and axial positions around tin center [24].

Many drugs presently in clinical use or advanced clinical trials have DNA as their pharmacological target [25]. The drug-DNA interaction study plays a vital role in designing and producing the new DNA-targeted drugs, and their efficiency depends on the mode and

affinity of the binding [26, 27] Tin complexes' interaction with DNA, damages cancer cells' DNA and prevents cell division, which results in cell death [17]. The binding ability with DNA of tin-based organic compounds depends primarily on the nature of the groups attached to the central Sn atom and the coordination number [28].

Various desirable characteristics of hydrazides include; their flexible structure, conjugated -system, easily hydrogen-bonding NH unit, and protonation-deprotonation site [29]. Hydrazone ligands have gained a lot of attention in the development of organotin anticancer drugs because of their favourable biological features and electron-donating atoms like carbonyl oxygen and imino nitrogen [30-33]. Because hydrazides can combine with metal ions to form coordination complexes, their biological activities as a free hydrazide ligand are enhanced [34].

This research paper reports the synthesis of N'-(3-ethoxy-2-hydroxybenzylidene)formohydrazide and its diorganotin(IV) complexes. The synthesized compounds were analyzed using FT-IR, ^{1}H-NMR, ^{13}C-NMR, Mass Spectrometer, and single crystal X-ray analysis. Their drug-DNA interaction mode was assessed by UV-visible spectroscopy, viscometry and electrochemical assay. The antioxidant activity against DPPH was also carried out and all compounds were tested for anticancer activity in order to investigate a potential relationship between DNA-binding capacity and toxicity against human breast cancer cell line MDA-MB-231 via MTT assay.

Experimental

Materials and methods

All the chemicals used were purchased from Alfa Aesar (Germany) including dimethyltin(IV) dichloride, dibutyltin(IV) dichloride, di-terbutyltin(IV) dichloride, diphenyltin(IV) dichloride, dioctyltin(IV) oxide, formic hydrazide and 3-ethoxysalisaldehyde. All the solvents were purchased from E. Merck (Germany). Solvents, including toluene and triethylamine, were

dried before use according to standard procedures [35]. The sodium salt of salmon sperm DNA (SS-DNA) was used as received (sigma). The melting points were determined using a melting point apparatus (model; MP-D, Mitamura Riken Kogyo) (Japan). The FT-IR spectra of all samples were recorded in the range of 4000-400 cm^{-1} on a Bruker Alpha II instrument. ^{1}H-NMR and ^{13}C-NMR spectra were obtained using $CDCl_3$ as a solvent on a Bruker Advance 300 (300 MHz) spectrometer. Single crystal analysis was done using a SuperNova Dual Source Single Crystal Diffractometer (Mo X-ray source). ASAP-ESI-Q Exactive Plus mass spectrometer was used to record mass spectra. UV-Visible absorption data were obtained on a Shimadzu UV-1800. Electrochemical studies (Cyclic voltammetry and DPV) were done using an EmStat2–PalmSens, (Netherland).

Synthesis and characterization of ligand (H_2L) and organotin(IV) complexes (1-5)

N'-(3-ethoxy-2-hydroxybenzylidene)formohydrazide (H_2L)

The ligand was synthesized by the addition of 2-hydroxy-3-ethoxybenzaldehyde (0.016 mol, 2.76 g) in ethanol (50 mL) containing formic hydrazide (0.016 mol, 1 g) followed by stirring and reflux for 2 hr. Then above mixture was cooled down at room temperature to obtain a pale white solid. (Scheme 1) [36].

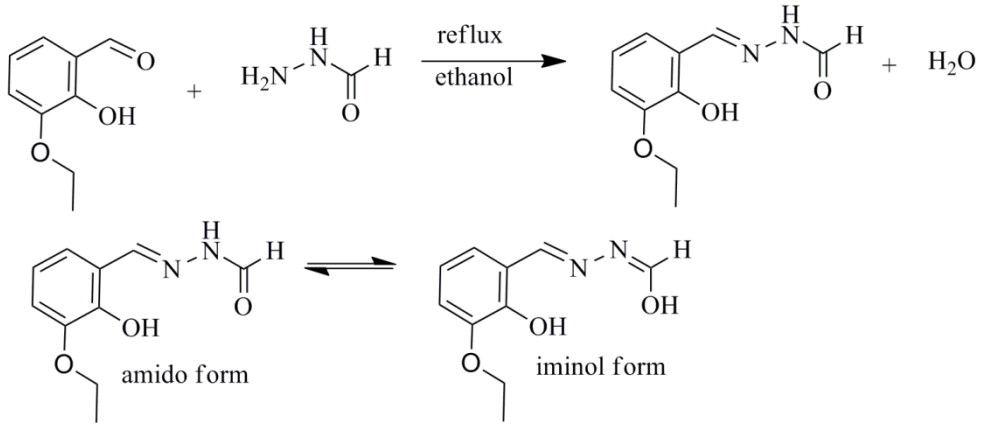

Scheme 1. Synthesis of N'-(3-ethoxy-2-hydroxybenzylidene)formohydrazide (**H_2L**)

Yield 90%, melting point: 180-182 °C. FT-IR (cm^{-1}): 3191 m ν(NH); 3047m ν(OH); 1738s ν(C=O); 1662s ν(C=N), 1048m ν(N-N). ^{1}H-NMR (ppm): H-3: 6.81 [d, ^{1}H, phenyl, $^{3}J_{H\text{-}H}$ =

7.8], H-4: 6.98 [t, ^{1}H, phenyl, $^{3}J_{H\text{-}H}$ = 7.8], H-5: 7.18 [d, ^{1}H, phenyl, $^{3}J_{H\text{-}H}$ = 6.9], H-7: 8.35 [s, ^{1}H, CH=N], H-8: 11.69 [s, 1H, CHO], H-9: 4.04 [q, ^{2}H, OCH_2, $^{3}J_{H\text{-}H}$ = 6.9], H-10: 1.34 [t, ^{3}H, O-C_2H_5 ,$^{3}J_{H\text{-}H}$ = 6.4], NH: 9.39 [s, ^{1}H, N-H], O-H: 10.53 [s, ^{1}H, O-H]. ^{13}C-NMR (ppm): C-7: 157.37 [HC=N], C-8: 165.18 [CONH], C-1-6: 147.81, 148.16, 118.59, 114.6, 120.57, 119.55 [Ph-C], C-9: 64.63 [O-CH_2], C-10: 15.10 [O-CH_2-CH_3]. ESI-MS, m/z calculated for $[C_{10}H_{12}N_2O_3+H]^+$ 209.0921, found 209.0921.

Dimethyltin(IV) [N-(3-ethoxy-2-oxidobenzylidene)-N′-(oxidomethylene)hydrazine] (1)

The ligand N'-(3-ethoxy-2-hydroxybenzylidene)formohydrazide (0.0024 mol, 0.5 g) and triethylamine (0.004 mol, 0.67 mL) were mixed with constant stirring for 10 min in toluene then Me_2SnCl_2 (0.0024 mol, 0.52 g) was added in the above mixture and stirred for 5-6 hr at room temperature (298 K), the yellowish product formed was filtered and recrystallized from chloroform and n-hexane mixture (1:4) (Scheme 2a, 2b).

Yield 93%, melting point: 90-92 °C. FT-IR (cm^{-1}): 1617s ν(C=N); 587m ν(Sn–O); 454w ν(Sn–N), 1048m ν(N-N); 1070m ν(N-N). ^{1}H-NMR (ppm): H-3: 6.93 [s, ^{1}H, phenyl], H-4: 6.57 [t, ^{1}H, phenyl, $^{3}J_{H\text{-}H}$ = 7.8], H-5: 6.95 [s, ^{1}H, phenyl], H-7: 8.62 [s, ^{1}H, CH=N] $^{3}J(^{119}$Sn-^{1}H) = 45 Hz, H-8: 7.53 [s, ^{1}H, N=CHO], H-9: 3.96 [q, ^{2}H, OCH_2, $^{3}J_{H\text{-}H}$ = 6.9], H-10: 1.29 [t, ^{3}H, O-C_2H_5 ,$^{3}J_{H\text{-}H}$ = 6.9], H-α: 0.65 [s, 6H, $2CH_3$], $^{2}J(^{119/117}$Sn-^{1}H) 79, 78 Hz. ^{13}C-NMR (ppm): C-7: 161.12 [HC=N], C-8: 163.76 [CO=N)], C-1-6: 150.45 156.45, 117.26, 115.93, 126.71 [Ph-C], C-9: 64.21 [O-CH_2], C-10: 15.41 [O-CH_2-CH_3], C-α: 7.25 $^{1}J[^{119/117}$Sn-^{13}C] = 650, 620 Hz. ESI-MS, m/z calculated for $[C_{12}H_{16}N_2O_3Sn + H]^+$ 357.01 found 357.02.

Dibutyltin(IV) [N-(3-ethoxy-2-oxidobenzylidene)-N′-(oxidomethylene)hydrazine] (2)

Complex (**2**) was synthesized using the same procedure as complex (**1**), but half the molar amounts (1: 2: 1) were used to form yellow crystals (Scheme 2a).

Yield 95%, melting point: 75-78 °C. FT-IR (cm^{-1}): 1601s ν(C=N); 554m ν(Sn–O); 434w ν(Sn–N); 1079m ν(N-N). ^{1}H-NMR (ppm): H-3: 6.76 [dd, ^{1}H, phenyl $^{3}J_{H\text{-}H}$ = 1.5, 9.5], H-4:

6.61 [t, ^{1}H, phenyl, $^{3}J_{H\text{-}H}$ = 7.9], H-5: 6.92 [dd, ^{1}H, phenyl $^{3}J_{H\text{-}H}$ = 1.4, 9.1], H-7: 8.62 [s, ^{1}H, CH=N] $^{3}J(^{119}Sn\text{-}^{1}H)$ = 40 Hz, H-8: 7.63 [s, ^{1}H, N=CHO], H-9: 4.05 [q, ^{2}H, OCH_2, $^{3}J_{H\text{-}H}$ = 6.9], H-10: 1.38 [t, ^{3}H, O-C_2H_5 ,$^{3}J_{H\text{-}H}$ = 7.0], H-α: 1.61-1.72 [m, 4H, $2CH_2$], H-β: 1.48-1.52 [m, 4H, $2CH_2$], H-γ: 1.25-1.33 [q, 4H, $2CH_2$, $^{3}J_{H\text{-}H}$ = 7.2], H-δ: 0.86 [t, 6H, $2CH_3$, $^{3}J_{H\text{-}H}$ = 7.2]. ^{13}C-NMR (ppm): ^{13}C-NMR (ppm): C-7: 162.99 [HC=N], C-8: 164.03 [CO=N], C-1-6: 150.55, 158.72, 116.34, 119.44, 126.66, 116 [Ph-C], C-9: 65.19 [O-CH_2], C-10: 15.07 [O-CH_2-CH_3], C-α: 22.72, C-β: 27.12, C-γ: 26.60, C-δ: 13.71. ESI-MS, m/z calculated for [$C_{18}H_{28}N_2O_3Sn$ + H]$^{+}$ 441.12, found 441.11.

Di-ter-butyltin(IV)[N-(3-ethoxy-2-oxidobenzylidene)-N′-(oxidomethylene)hydrazine] (3)

Complex (**3**) was synthesized using the same procedure as complex (**2**), using identical molar amounts, to form yellow crystals (Scheme 2a).

Yield 89%, melting point 86-88 °C. FT-IR (4000-400 cm^{-1}): 1604s ν(C=N); 588m ν(Sn–O); 525w ν(Sn–N); 1082m ν(N-N). ^{1}H NMR (ppm): H-3: 7.00 [dd, ^{1}H, phenyl, $^{3}J_{H\text{-}H}$ = 1.8, 9.3], H-4: 6.60 [t, ^{1}H, phenyl, $^{3}J_{H\text{-}H}$ = 7.8], H-5: 7.04 [dd, ^{1}H, phenyl, $^{3}J_{H\text{-}H}$ = 1.5, 9.6], H-7: 8.88 [s, ^{1}H, CH=N] $^{3}J(^{119}Sn\text{-}^{1}H)$ = 49 Hz, H-8: 7.76 [s, ^{1}H, N=CHO], H-9: 4.01 [q, ^{2}H, O-CH_2, $^{3}J_{H\text{-}H}$ = 6.9], H-10: 1.29 [t, ^{3}H, O-CH_2-CH_3 ,$^{3}J_{H\text{-}H}$ = 7.0], H-β: 1.25 [s, 18H, $6CH_3$] $^{3}J(^{119/117}Sn\text{-}^{1}H)$ = 110, 105 Hz. ^{13}C NMR (ppm): C-7: 163.38 [HC=N], C-8: 164.03 [CO=N], C-1-6: 150.37, 159.52, 117.06, 116.36, 127.44, 117.06 [Ph-C], C-9: 65.17 [O-CH_2], C-10: 15.46 [O-CH_2-CH_3], C-α: 40.14, C-β: 29.57. ESI-MS, m/z calculated for [$C_{18}H_{28}N_2O_3Sn$ + H]$^{+}$ 441.12, found 441.11.

Diphenyltin(IV) [N-(3-ethoxy-2-oxidobenzylidene)-N′-(oxidomethylene)hydrazine] (4)

Complex (**4**) was synthesized using the same procedure as complex (**2**), using identical molar amounts, to form yellow crystals (Scheme 2a).

Yield 84%, melting point 150-152 °C. FT-IR (4000-400 cm^{-1}): 1601s ν(C=N); 581m ν(Sn–O); 473w ν(Sn–N);1074m ν(N-N). ^{1}H NMR (ppm): H-3: 7.02 [d, ^{1}H, phenyl, $^{3}J_{H-H}$ = 4.8], H-4: 6.63 [t, ^{1}H, phenyl, $^{3}J_{H-H}$ = 7.8], H-5: 7.04 [d, ^{1}H, phenyl, $^{3}J_{H-H}$ = 4.5], H-7: 8.63 [s, ^{1}H, CH=N] $^{3}J(^{119}Sn\text{-}^{1}H)$ = 40 Hz, H-8: 8.32 [s, ^{1}H, N=CHO], H-9: 4.07 [q, ^{2}H, O-CH_2, $^{3}J_{H-H}$ = 6.9], H-10: 1.43 [t, ^{3}H, O-CH_2-CH_3 ,$^{3}J_{H-H}$ = 6.9], H-β: 7.72-7.79 [m, ^{4}H, phenyl], H-γ, H–δ: 7.32-7.61 [m, 6H, phenyl]. ^{13}C NMR (ppm): C-7: 159.61 [HC=N]; C-8: 163.40 [CO=N], C-1-6: 146.64, 150.71, 117.96, 116.55, 135.11, 119.36 [Ph-C], C-9: 64.87 [O-CH_2], C-10: 15.50 [O-CH_2-CH_3], C-α: 135.11, C-β: 129.41, C-γ: 128.77, C-δ: 127.23. ESI-MS, m/z calculated for $[C_{22}H_{20}N_2O_3Sn + H]^{+}$ 480.12, found 480.05.

Dioctyltin(IV) [N-(3-ethoxy-2-oxidobenzylidene)-N'-(oxidomethylene)hydrazine] (5)

N'-(3-ethoxy-2-hydroxybenzylidene)formohydrazide (0.0024 mol, 0.5 g) and dioctyltin(IV) oxide (0.0024 mol, 0.86 g) were mixed in toluene (100 mL), the resulting yellow solution was refluxed for 6 hr until the solution became clear. Using the Dean and Stark Apparatus, water formed as a by-product during reaction water was removed. The solvent was removed using a rotary evaporator, and a yellow oily product was obtained (Scheme 2c).

Yield 77%, Viscous liquid. FT-IR (4000-400 cm^{-1}): 1604s ν(C=N); 590m ν(Sn–O); 430w ν(Sn–N); 1087 ν(N-N). ^{1}H NMR (ppm): H-3: 6.91 [s, ^{1}H, phenyl], H-4: 6.53 [t, ^{1}H, phenyl, $^{3}J_{H-H}$ = 7.8], H-5: 6.93 [s, ^{1}H, phenyl], H-7: 8.67 [s, ^{1}H, CH=N] $^{3}J(^{119}Sn\text{-}^{1}H)$ = 46 Hz, H-8: 7.58 [s, ^{1}H, N=CHO], H-9: 3.97 [q, ^{2}H, O-CH_2, $^{3}J_{H-H}$ = 6.9], H-10: 1.28 [t, ^{3}H, O-CH_2-CH_3 ,$^{3}J_{H-H}$ = 6.9], H-α: 1.41-1.48 [m, ^{4}H, 2CH_2], H-β: 1.30-1.36 [m, ^{4}H, 2CH_2], H-γ - γ': 1.12-1.17 [bs, 16H, 2CH_2 CH_2CH_2 CH_2], H-δ': 0.81 [t, 6H, 2CH_3, $^{3}J_{H-H}$ = 7.2]. ^{13}C NMR (ppm): C-7: 161.70 [HC=N], C-8: 164.05 [CO=N], C-1-6: 150.36, 158.04, 117.19, 115.69, 126.90, 118.31 [Ph-C], C-9: 64.935 [O-CH_2], C-10: 14.36 [O-CH_2-CH_3], C-α: 22.54, C-β: 24.74, C-γ: 32.96,

C-δ: 29.01, C-α': 28.97, C-β': 31.69, C-γ': 26.09, C-δ': 14.36. ESI-MS, m/z calculated for $[C_{26}H_{44}N_2O_3Sn + H]^+$ 552.36, found 551.24.

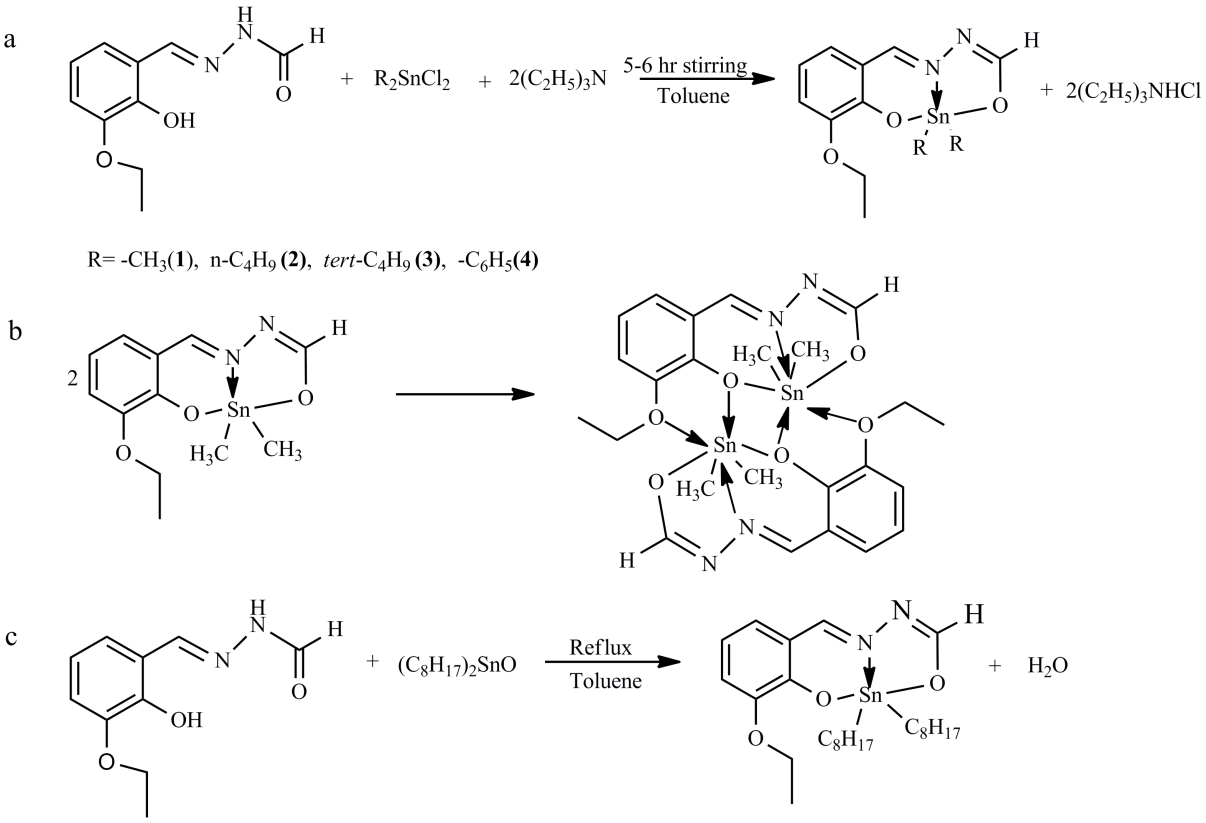

Scheme 2. Synthesis of diorganotin(IV) complexes (a-c)

DNA Binding studies

Absorbance spectroscopic studies

The SS-DNA solution was made by adding SS-DNA (4 mg) into distilled water (50 mL) and was dissolved by stirring overnight, then the solution was stored at 4 °C. The purity of the SS-DNA solution was determined by taking the ratio of UV absorbance at 260 and 280 nm and was about 1.8, indicating the DNA is pure [25, 37, 38]. The concentration of the DNA solution was found using the UV-VIS spectrometer and applying the Beer-Lambert Law on obtained data, taking the molar absorption coefficient (ε) value of 6,600 $M^{-1}cm^{-1}$ (260 nm) for SS-DNA. The solution concentration was found to be 2×10^{-4} M [27]. The solution (0.1 mM)

of synthesized compounds were prepared by dissolving in 70% DMSO. The concentration of the synthesized compound was kept constant for DNA interaction studies, while the concentration of SS-DNA was varied from 5-25 μM. The total volume of the compound solution was kept constant. The resulting solutions were kept at constant temperatures of 298 K and 310 K for 10 min before taking spectroscopic measurements, quartz cuvettes of path length 1 cm were used to record absorption spectra [39].

Viscosity measurements

The SS-DNA solution (25 μM) was taken in a viscometer and the concentrations of ligand (**H_2L**) and organotin (IV) complexes (**1-5**) were varied (0-25 μM) at constant temperature (37 ± 1°C) in a thermostated bath. A digital stopwatch was used to measure the flow time for the samples. The measurements were done in triplicate for each sample. Viscosity graph, $(\eta/\eta_o)^{1/3}$ vs. binding ratio ([compound]/[DNA]) was plotted, where η_o is the viscosity of free DNA and η is the viscosity of DNA in the presence of compounds. The viscosity value was determined by equation ($\eta_o = t - t_o$) while t is the time of flow of SS-DNA in the absence or presence of compounds and t_o is the flow time of distilled water [39-41].

Electrochemical assay

To obtain voltammograms of synthesized sample solutions in 70% DMSO, a three-electrode cell was used, with 0.1 M TBAP (tetrabutylammonium perchlorate) as a supporting electrolyte. The working electrode was glassy carbon (GC) electrode, Pt wire was used as a counter electrode, and saturated silver/silver chloride (Ag/AgCl) as a reference electrode. The surface area of the GC is 0.03 cm^2. The working electrode (GC) was cleaned before and after the experiment by rubbing on a nylon buffing pad with an alumina powder (Al_2O_3) aqueous suspension at room temperature (25 °C). Throughout the experiments, a scan rate of 100 mV/s was used. Purging of the sample solution was done before every electrochemical measurement with argon gas to exclude any reactive oxygen. The conditions for differential

pulse voltammetry were pulse amplitude 50 mV, pulse width 70 ms and scan rate of 50 mVs^{-1} [42].

DPPH free radical scavenging assay

The synthesized compounds were screened for DPPH (2,2-diphenyl-1-picrythydrazyl) free radical scavenging ability using a previously reported procedure [43]. The DPPH stock solution (255 µM) was prepared in 100 mL of methanol and was kept in dark for 30 min. The stock solution of synthesized compounds (50 µM) was also prepared in methanol. The stock solutions of ligand and organotin(IV) complexes were diluted to 20, 40, 60, 80, and 100 µM, followed by the addition of 1 mL of 255 µM DPPH to each diluted concentration. Then this mixture was properly mixed and incubated for 30 min in dark at room temperature. An aliquot (250 µL) of each mixture was added in triplicates to a 96-welled microplate. The microplate reader (model 680-BIO-RAD, USA) was used to measure the absorbance of these mixtures at a wavelength of 515 nm. For positive control, ascorbic acid was used over a similar concentration range. All measurements were done in triplicates. The percentage scavenging properties estimated from the DPPH assay methods was obtained using the following equation in (1)

$$(\%)\ \text{inhibition} = [\ (A_c - A_t)\ /A_c] \times 100 \qquad (1)$$

where A_c = absorbance of the positive control, and A_t = absorbance of the test compound.

Cytotoxic activity

Cell culture

Human breast cancer cell line (MDA-MB-231) was grown in standard culturing conditions. Briefly, the cells were grown in Dulbecco's Modified Eagle Medium (DMEM) containing 10% Fetal Bovine Serum (FBS) and 1% penicillin-streptomycin at 37ºC and 5% CO_2.

In vitro anticancer assay

The cytotoxic potentials of the newly synthesized ligand (**H_2L**) and its organotin(IV) complexes (**1–5**) on the breast cancer cell line (MDA-MB-231) were assessed by using (3-(4,5-dimethylthiazolyl-2)-2,5-diphenyltetrazolium bromide) MTT assay [44]. The cells were seeded in 96 well plates 24 hr prior to the treatments in triplicate. The test compounds were dissolved in 0.1% DMSO and diluted to different concentrations (0, 10, 20, 40, 80, 100, 150, 200 µg/mL). For control, 0.1% DMSO was used. After 48 hours of exposure to the compounds, an equal volume of MTT solution was added to the existing media in each well. After 3 hrs of incubation at 37°C, 150 µL of MTT solvent (4 mM HCl, 0.1% NP40 in isopropanol) was added in each well, shaken for 15 minutes and absorbance was measured at 590 nm. Cisplatin was used as positive control [44]. The results were expressed as percentage of viable cells against the concentration of compounds.

Results and discussion

FT-IR Spectroscopy

FT-IR spectral data of synthesized ligand (**H_2L**) and its organotin (IV) complexes (**1-5**) were recorded in the range of 4000-400 cm^{-1}. In the FTIR spectrum of ligand N'-(3-ethoxy-2-hydroxybenzylidene)formohydrazide, the main vibrational bands observed were at 3197 cm^{-1} ν(N-H), 3047 cm^{-1} ν(O-H), 1662 cm^{-1} ν(C=O) and 1605 cm^{-1} ν(C=N). When complex is formed, deprotonation and enolization of the ligand (**H_2L**) occur, resulting in disappearance of these bands. The band due to ν(C=N) also shifts to 1617-1601 cm^{-1} indicating coordination of azomethine nitrogen with the Sn atom. Due to complex formation, the shift in the ν(N-N) band from 1048 cm^{-1} to 1070-1087 cm^{-1} is witnessed, indicating a reduction in repulsive force of the lone pairs of electrons on the nitrogen atoms [43]. In the 554-590 cm^{-1} and 408-454 cm^{-1} range, new bands appeared assigned to ν(Sn-O) and ν(Sn-N), respectively. The appearance of these bands confirmed the synthesis of the new organotin(IV) complexes [45]. According to analysis of the IR spectra, the ligand attach to the tin metal in tridentate form.

NMR spectroscopy

The spectra of ^{1}H-NMR showed signals at 10.53 and 9.39 owed to –OH and –NH protons, respectively and these signals were not present in the spectra of organotin(IV) complexes (**1-5**) because aldo-imine form of ligand was converted to imine-ol form followed by deprotonation. Due to coordination of azomethane nitrogen (CH=N) with tin atom down field shift 8.58-8.88 ppm in the resonance signal of its proton was observed with the coupling constant of ^{3}J (^{119}Sn, ^{1}H) value of 36-51 Hz. All other protons of the synthesized ligand (**H_2L**) and complexes (**1-5**) resonates in the expected region. The coupling constant of ^{2}J ($^{119/117}$Sn, ^{1}H) for complex (**1**) was observed to be 79 Hz and furthermore from Lockhart's equation $\theta = 0.0161\,[^{2}J]^{2} - 1.32\,[^{2}J] + 133.4$ the angel of C-Sn-C angle in solution was found to be 129.6°, which confirms that in solution state Sn atom is penta coordinated [46]. The ^{1}H-NMR confirms that the Schiff base is tridentately linked to the tin metal [32, 45, 47]. The signals observed in ^{13}C-NMR spectra of all complexes are in conformation with the anticipated composition.

Mass spectrometry

The molecular weight of the substances is determined by the mass spectra. The ligand (**H_2L**) and its complexes (**1-5**) showed molecular ion peak of significant intensity with the characteristic peak pattern of Sn. Presence of the characteristic tin isotopic peak pattern in the various fragments of complexes (**1-5**) showed successful binding of Sn with the ligand. As complex (**1**) was dinulear (confirmed from XRD), its mass spectrum showed a small peak at m/z 709, corresponding to dinuclear specie, where as a peak at m/z 357.01 was also present corresponding to the mononuclear fragment of the complex (**1**) [48]. The fragments $[C_{10}H_{12}N_2O_3]^{+}$ 209.09, $[C_9H_{10}NO_2]^{+}$ 164.07 and $[C_7H_5NO_2]^{+}$ 136.04 were observed in the mass spectra of all compounds.

X-Ray single crystal analysis

Complex (**1**) is a binuclear complex consisting of the asymmetric unit, half of the dimer. The atomic numbering and molecular structure for complex (**1)** molecule are given in Fig.1. The selected bond lengths, bond angles, and the crystallographic data of the di-nuclear complex (**1)** are given in Tables 1 and 2. In the di-nuclear complex, a four-membered planer Sn_2O_2 ring is present. The Sn1-O1A and Sn1-O2 bond distances are 2.574(3) and 2.201(3) Å respectively. The two formula units in each dinuclear molecule are bridged together through the ethoxy and phenolic oxygen atoms. The Sn1 atom and O(1A), C(1), C(6), C(7), N(1) atoms form a six membered ring, while Sn1, O(2), C(8), N(2), N(1) and Sn1, O(1A), C(1), C(2A), O(3A) atoms form five membered rings. Each $(CH_3)_2Sn(IV)$ moiety is bonded to four oxygen atoms and nitrogen, forming an O_4NC_2 core around the tin atom. Due to steric requirements of the five- and six membered rings, the ligand is non-planar. The angle between C10-Sn1-C9 is 164.8(2)°, and the geometry around the Sn atom can be characterized as a distorted pentagonal bipyramidal. The packing diagram offers a wavy supramolecular structure for complex (**1**) mediated by H7···N2 (2.554 A) intermolecular non-covalent interactions (Fig. 2). The adjacent wavy layers are connected to one another via H9···C8 (2.845 Å) interactions (Fig. 2). These interactions are comparable with the already reported in literature [48].

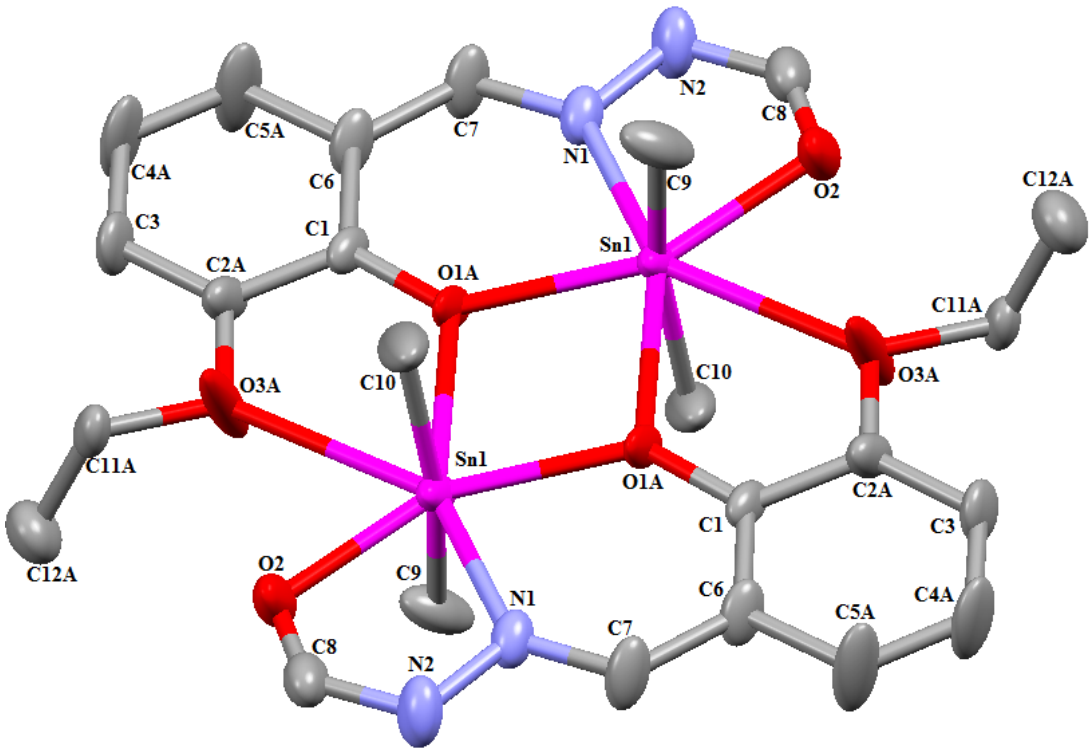

Fig. 1 Molecular structure of dimethyltin(IV) complex (**1**)

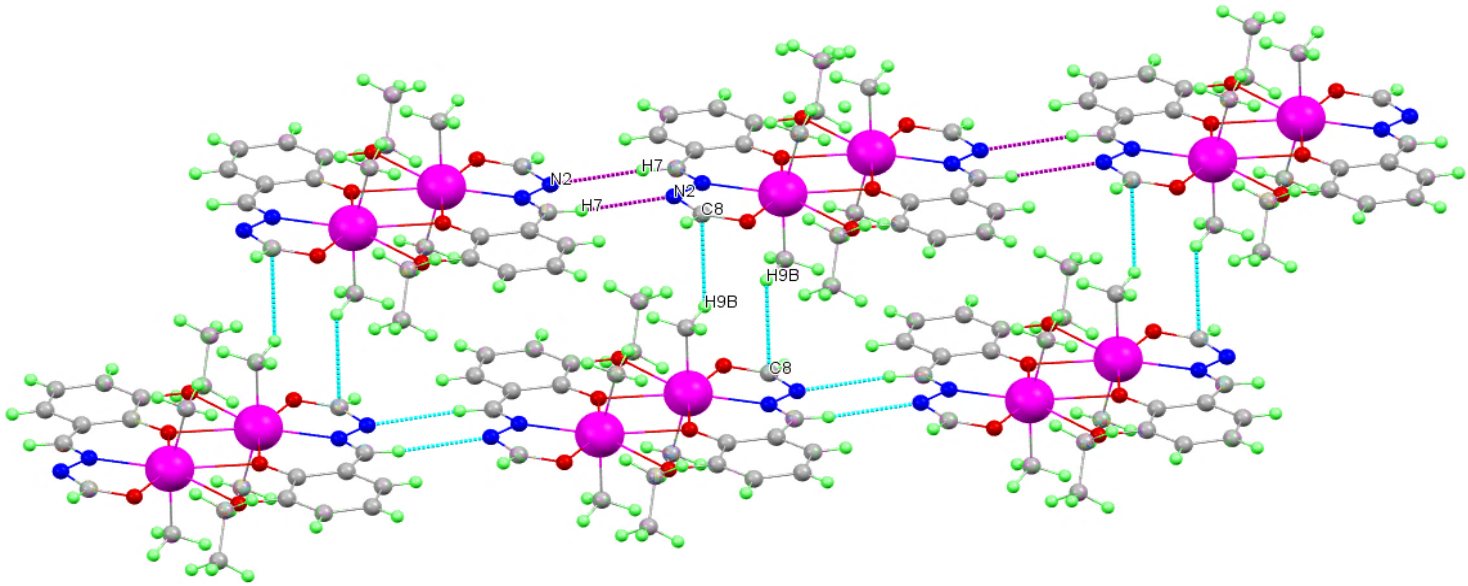

Fig. 2 Supramolecular single wavy layer of complex (**1**) mediated by N2···H7 intermolecular non-covalent interactions and two wavy layers are connected through C8···H9B interactions (blue dotted lines).

Table 1 Bond lengths (Å) and bond angles (°) data of complex (**1**)

Bond Lengths (Å)			
Sn1-O1A	2.574 (3)	Sn1-N1	2.228 (3)
Sn1-O1A	2.220 (3)	Sn1-C9	2.103 (7)
Sn1-O3A	2.636 (4)	Sn1-C10	2.100 (6)
Sn1-O2	2.201 (3)		
Bond Angles (°)			
O1A-Sn1-O2	152.8(1)	O2-Sn1-O1A	133.1(1)
O1A-Sn1-N1	81.6(1)	O2-Sn1-N1	71.2(1)
O1A-Sn1-C9	93.4(2)	O2-Sn1-C9	91.2(2)
O1A-Sn1-C10	93.1(2)	O2-Sn1-C10	89.2(2)
O1A-Sn1-O3A	135.2(1)	O2-Sn1-O3A	71.9(1)
O1A-Sn1-O3A	61.2(1)	C9-Sn1-C10	164.8(2)
O1A-Sn1-O1A	74.0(1)	C9-Sn1-O1A	84.3(2)
N1-Sn1-C9	97.0(2)	C9-Sn1-O3A	83.0(2)
N1-Sn1-C10	97.5(2)	C10-Sn1-O1A	84.3(2)
N1-Sn1-O3A	143.2(1)	C10-Sn1-O3A	82.7(2)
N1-Sn1-O1A	155.6(1)		

Table 2 Crystal data and structure refinement parameters for complex (**1**)

Parameters	**Complex 1**
Empirical formula	$C_{12}H_{17}N_2O_3Sn$
Formula weight	355.96
Temperature/K	150
Crystal system	Monoclinic
Space group	$P2_1/c$
a/Å	9.39130(10)
b/Å	14.4742(2)
c/Å	10.03260(10)
α/°	90
β/°	103.4230(10)
γ/°	90
Volume/Å^3	1326.49(3)

Z	4
ρ_{calc}g/cm^3	1.782
μ/mm^{-1}	15.363
F(000)	708.0
Crystal size/mm^3	0.295 × 0.253 × 0.244
Radiation	CuKα (λ = 1.54184)
Reflections collected	24235
Independent reflections	2618 [R_{int} = 0.0418, R_{sigma} = 0.0158]
Data/restraints/parameters	2618/59/186
Goodness-of-fit on F^2	1.039
Final R indexes [I>=2σ (I)]	R_1 = 0.0375, wR_2 = 0.0834
Final R indexes [all data]	R_1 = 0.0380, wR_2 = 0.0837
Largest diff. peak/hole / e Å^{-3}	1.45/-1.87

DNA Binding studies

Absorption spectroscopic studies

The mode of interaction and binding strength of synthesized organotin(IV) complexes with SS-DNA were investigated using a UV-visible spectrometer. The changes in the electronic spectra of synthesized ligand (**H_2L**) and its organotin(IV) complexes (**1-4**) were observed by varying concentrations of SS-DNA (5-25 μM), (Fig. 3). The tri-dentate ligand [N'-(3-ethoxy-2-hydroxybenzylidene)formohydrazide] showed broad bands of absorption due to the π-π* and n-π* energy-levels excitations in the visible region (350-470 nm) [45].

Due to Compound-DNA interactions, a hypochromic effect, i.e., decrease in peak intensity, and red shift in wavelength in the range of 2-8 nm for all compounds, is observed. The interaction between the complex and the DNA results in a change in the conformation of the molecule, which is the cause of hypochromism. The binding force affects the spectrum in a way that makes the hypochromism more pronounced when stronger the effect is [49]. As

reported in the literature, an intercalative mode of interaction is indicated in this case of drug-DNA interaction due to the presence of both hypsochromic and hypochromic effects simultaneously [39, 43, 49].

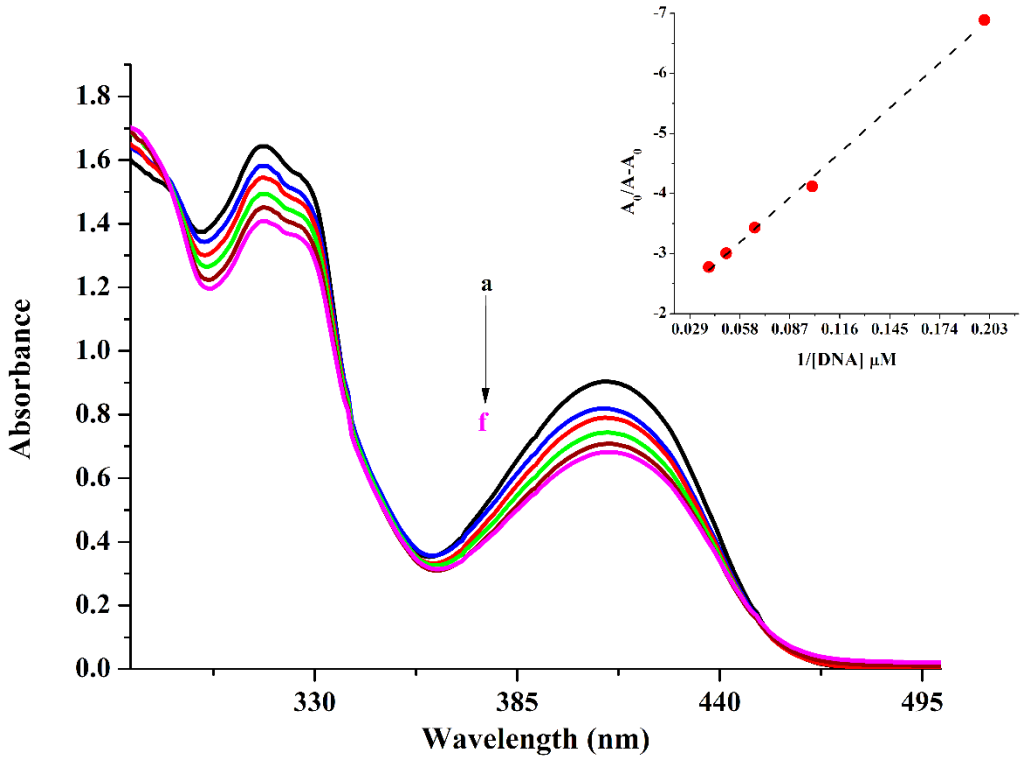

Fig. 3 Absorption spectra of 0.1 mM of complex (**1**) in absence (a) and presence of 5 (b), 10 (c), 15 (d), 20 (e), 25 (f) µM DNA. The arrow indicates the increasing conc. of DNA. The inset graph represents the plot of Ao/A-Ao vs. 1/[DNA] $(\mu M)^{-1}$ for the calculation of binding constant (K_b).

Using Benesi-Hildebrand equation (eq. 2) binding constant K can be calculated from the variation in peak intensity data of all compounds [36].

$$\frac{A_0}{A-A_0} = \frac{\varepsilon_G}{\varepsilon_{H-G}-\varepsilon_G} + \frac{\varepsilon_G}{\varepsilon_{H-G}-\varepsilon_G} \times \frac{1}{K_b[DNA]} \quad (2)$$

Where A_o and A are the absorptions and ε_G and $\varepsilon_{H\text{-}G}$ are the molar-extinction coefficients of free complex and complex-DNA adducts, where K_b is the binding constant.

Using the intercept to slope ratio from the graph (Fig. 3) of $A_o/(A\text{-}A_o)$ vs. 1/[DNA], the binding constant value K_b was calculated and is reported in Table 3. The observed order of binding constant values was (**2**) > (**3**) > (**4**) > (**1**) at temperature 298 K and the K_b values (the order of 10^4 $L{\cdot}mol^{-1}$) that were observed agreed well with those that had been reported for comparable intercalated metal-complexes [50-52]. Complex (**2**) showed the highest binding constant value (9.64×10^4) at 298 K, this confirms its efficacy as a prospective cancer chemotherapeutic medication candidate. The greater value of K_b for butyl derivatives is due to formation of additional hydrophobic interactions with the nucleotide bases [49]. The SS-DNA and these complexes interacted strongly, as indicated by the relatively high K_b content and red shift.

The molar (ΔG°) Gibb's free energy was also calculated using the following equation

$$\Delta G = -RT \ln K_b \quad (3)$$

Where R = (8.314 J K^{-1} mol^{-1}) and T is the temperature in Kelvin (298 K). The formation of complex-DNA adduct is a spontaneous process as the ΔG° value observed for the synthesized compounds is negative.

Enthalpy (ΔH) and entropy (ΔS) values were calculated by using equation (4) and (5) [53].

$$-\Delta H = \frac{RT_1T_2 \ln \left(\frac{K_2}{K_1}\right)}{T_2 - T_1} \quad (4)$$

$$\Delta G = \Delta H - T\Delta S \quad (5)$$

The enthalpy (ΔH) value was positive, so the endothermic nature of the reaction is indicated. The positive value of entropy (ΔS) for DNA-Drug adduct formation is due to distortions of the DNA helix, as shown in Table 3 [54].

Table 3 Thermodynamic data and binding constants of **H_2L** and its derivatives (**1-4**)

Complexes	K_b	ΔG (kJ/mol)	ΔH (kJ)	ΔS (kJ/K)
H_2L	3.28×10^4	-20.1	30.45	0.17
1	3.62×10^4	-26.0	17.52	0.15
2	9.64×10^4	-28.4	1.58	0.10
3	8.83×10^4	-28.2	2.30	0.10
4	4.43×10^4	-26.5	9.35	0.12

Viscosity measurement

To confirm the DNA binding mode, the compound's interactions with the SS-DNA were also studied by viscometry. Viscosity measurements are affected by variation in the length of DNA helix and are known to be reliable experiments for determining the binding mode. In intercalative mode of binding, an increase in the viscosity of the DNA solution was observed, which is due to the attachment of binding compounds between the base pairs of the DNA helix. On the other hand, in the case of a non-classic intercalation binding model, the compound binds in the DNA grooves, causing bending of the DNA helix and decreasing its length. In contrast, the viscosity of DNA solution remains unchanged/reduced [55, 56].

Fig. 4 shows a graph of $(\eta/\eta_o)^{1/3}$ vs. [compound]/[DNA] which provides an extent of change in viscosity. From Fig. 4, it can be observed that with the addition of synthesized compounds into the DNA solution, relative viscosity of DNA increases suggesting the nature of binding of the compounds is intercalative [57].

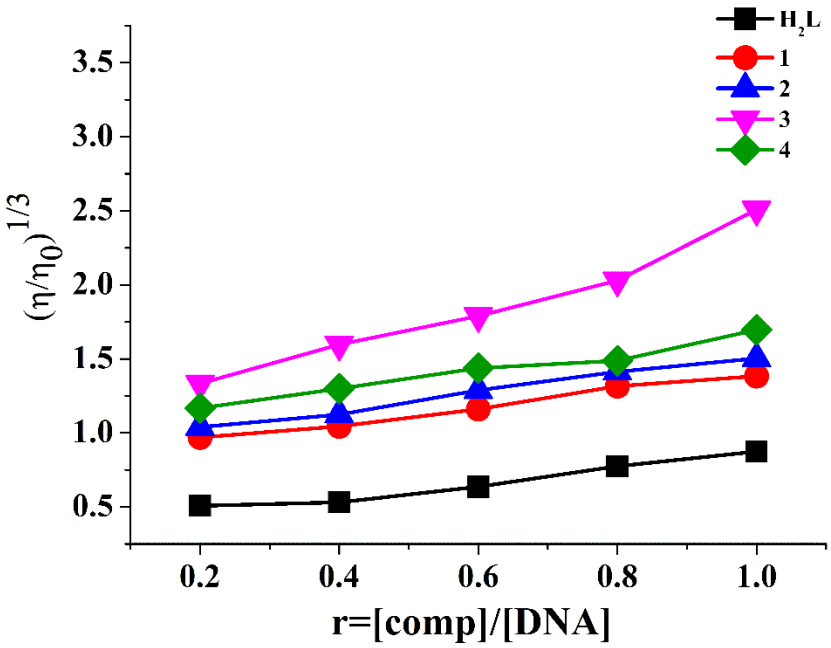

Fig. 4 Effect of increasing amounts of **H_2L** and complexes (**1-4**) on relative viscosity of SS-DNA at 37 ± 0.1 °C. [DNA] = 1.4×10^{-4} M, r = 0.2, 0.4, 0.6, 0.8, 1.

Electrochemical assay

Cyclic voltammetry

The electrochemistry of the synthesized complexes (**1-4**) in 70% DMSO solution was done using cyclic voltammetry (CV). Firstly, the CV of the synthesized compounds in the absence of SS-DNA were carried, and the reduction peak for complexes (**1**), (**2**), (**3**), and (**4**) was observed around -1.60 V, -1.67 V, -1.65 V, -1.50 V, respectively, which can be attributed to the reduction of tin Sn^{+4}/Sn^{+2} state (Fig. 5). The broadness of the cathodic peak of all these complexes may be due to the overlapping of two reduction peaks, each contributing 1e as directed by equation $[E_p\text{-}E_{p/2}] = 70$ mV [45]. The irreversible nature of the system is indicated by the absence of an anodic peak in the reverse scan (Fig 5).

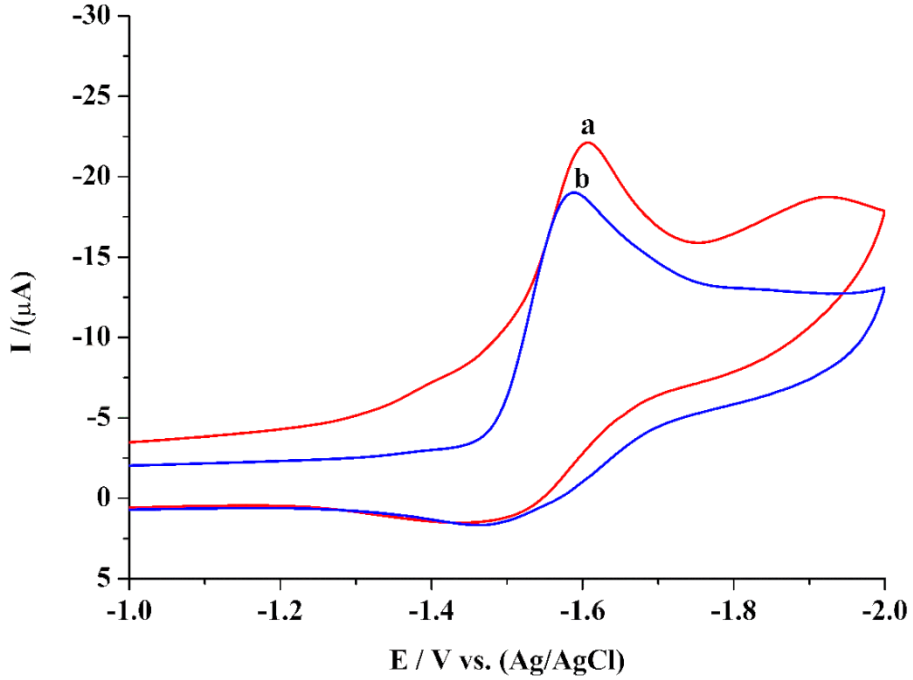

Fig. 5 Cyclic voltammogram of complex (**1)** in the (a) absence and (b) presence of 100 μM SS-DNA

The cyclic voltammograms were also recorded after adding 20-100 μM SS-DNA solution in diorganotin(IV) complexes (**1-4**) solutions with constant concentration (3×10^{-3} M). Due to drug-DNA adduct formation, specific changes in electrochemical response for the complexes and respective current-potential parameters were observed. In the presence of SS-DNA (100 μM) in the complex solution, the CV of organotin(IV) complex (**1-4**) showed a 31.00%, 22.36%, 42.62%, and 22.69%, decline in the cathodic peak current (I), respectively. The positive shift of 15 mV, 20 mV, 15 mV, 35 mV in peak potential was also observed along with the decline for the synthesized complexes, respectively, as depicted in Fig 5. Both observations indicate the intercalative mode of interaction of DNA with the complex molecules [45, 54, 58, 59].

Using Randlese Sevcik equation (6) for irreversible process, a Plot of cathodic peak current (I) vs. the square root of the scan rate ($\upsilon^{1/2}$) in the absence and presence of DNA for complex

(**1-4**) were plotted. This plot helps determine the electrochemical process mechanism, i.e., adsorption controlled or diffusion-controlled [45, 60, 61].

$$I = 2.99 \times 10^5\, n\, (\alpha n)^{1/2}\, A C_o^{*}\, D^{1/2}\, \upsilon^{1/2} \quad (6)$$

Where I (A) is peak-current, α = 0.5 is the transfer coefficient, A (cm^2) is the electrode's surface area, D ($cm^2\ s^{-1}$) is the diffusion coefficient, Co* (mol cm^{-3}) is the concentration of the electro-active species and υ (V s^{-1}) is the scan rate.

Plots for all complexes were found to be linear in both cases, i.e., before and after adding SS-DNA, and the linearity of the plots determines that the primary mass transport to the surface of the electrode is diffusion-controlled of these complexes (Fig. 6a) and their DNA adducts (Fig. 6b) [45]. In the presence of DNA, the diffusion of redox species is slower, as evident from the lower diffusion coefficient values of complex (**1-4**), and is the reason for the decrease in peak currents of cyclic-voltammograms (Fig. 5).

Using equation 7, the stability constant (K) value for Complex-DNA adduct was also determined [61].

$$1/[\mathrm{DNA}] = \frac{K(1-A)}{(1-\frac{I}{I_0})} - K \quad (7)$$

Where A is a constant. The stability constant or binding constant K values were determined from a CV and are in the order of complex (**2**) > (**3**) > (**4**)> (**1**) the trend is similar to that found from the UV-visible spectroscopic data (Table 3). The higher K value of complex (**2**) and (**3**) than complex (**4**) and (**1**) is due to the butyl group, which forms additional hydrophobic interactions with the nucleotide bases [45].

For calculating the number of binding sites, equation 8 was used (Table 4).

$$C_b/C_f = K[\mathrm{DNA}]/2s \quad (8)$$

Where C_f is the conc. of free species and C_b is the DNA-complex bound species, s is the number of binding sites in terms of the concentration of base pairs. C_b/C_f can be also be

represented by equation [63]. The binding site's size data showed that all the complexes (**1-4**) interact with more base pairs of the SS-DNA. These results indicated that complexes have stronger interactions with DNA and can be used as potential anticancer drugs.

Standard Gibbs free energy ($\Delta G = -RT \ln K$) values were also calculated through K_b data and were found to be negative. The data indicated that these complexes-DNA interaction is spontaneous.

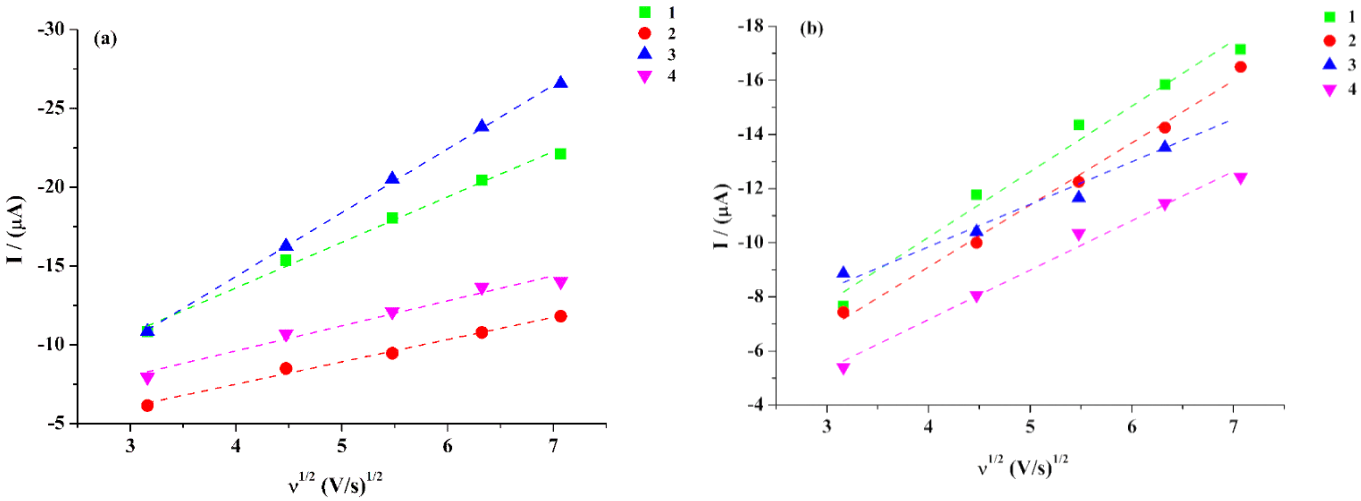

Fig. 6 Randlese Sevcik plot in the (**a**) absence of DNA **(b)** presence of DNA

Table 4 Cyclic voltammetry data of organotin (IV) complexes (**1-4)**

Complex	D_o (cm^2s^{-1}) (without DNA)	D_o (cm^2s^{-1}) (with DNA)	K_b(M^{-1}) (CV)	s (bp)	ΔG (kJ/mol)
1	1.21×10^{-8}	1.00×10^{-8}	4.44×10^{4}	4.19	-26.51
2	8.97×10^{-9}	3.42×10^{-9}	8.71×10^{4}	11.77	-28.18
3	1.24×10^{-8}	8.95×10^{-9}	8.04×10^{4}	10.05	-27.98
4	3.97×10^{-9}	3.69×10^{-9}	5.56×10^{4}	9.27	-27.07

Differential pulse voltammetry

Differential pulse voltammograms of the Complex (**1**) are presented in Fig. 7. For all the organotin (IV) complexes the observed $W_{1/2}$ values are approximately equal to 200 mV which suggest a two-electron transfer process. These values are larger than the theoretical value of 90 mV for an electron transfer process, which may be due to an uncompensated solution resistance.

In presence of SS-DNA (100 μM) in the solution the voltammogram (DPV) of diorganotin(IV) complex (**1-4**), showed a decrease in peak intensity, as well as a shift to a more positive potential, was observed similar to the CV data as shown in Table 5. Hence DPV data also support the intercalative mode of DNA interaction [64, 65].

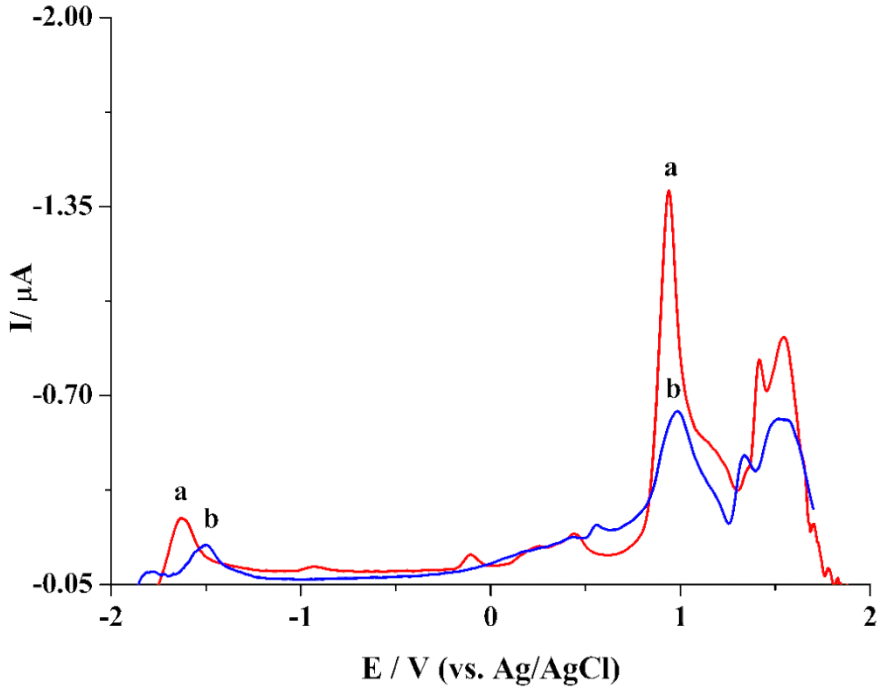

Fig. 7 Differential pulse voltammograms of a complex (**1**) (a) absence of SS-DNA (b) presence of SS-DNA. Pulse amplitude 50 mV, pulse width 70 ms, scan rate 50 mV s^{-1}

Table 5 Differential pulse voltametric parameters of complexes (**1-4**)

Complexes	Scan rate/Vs^{-1}	Epc/(V)	Shift in	I/µA	% Decrease in
1	0.5	-1.65		-0.27	
1-DNA	0.5	-1.50	14.50	-0.19	29.54
2	0.5	-1.64		-0.33	
2-DNA	0.5	-1.63	1.00	-0.22	33.51
3	0.5	-1.59		-0.31	
3-DNA	0.5	-1.58	1.00	-0.20	33.99
4	0.5	-1.48		-0.29	
4-DNA	0.5	-1.45	3.00	-0.17	38.93

DPPH free radical scavenging assay

The diorganotin(IV) complexes (**1-5)** have been studied for their ability to reduce the stable radical of 2,2-diphenyl-1-picrylhydrazyl (DPPH) by transferring the hydrogen atom, resulting in the formation of diphenylpicrylhydrazine and phenoxyl radicals, which can then undergo reactions like coupling, fragmentation, and addition. A colour change from violet to yellow occurs during the reaction which can be observed spectrophotometrically by measuring the decline in absorbance at 515 nm for 30 min [43]. The amount of antioxidants required to reduce the initial concentration of DPPH by 50% was measured as antioxidant activity (IC_{50}). The IC_{50} values for (**1–5**) varied between 47 and 89 µg/mL (Table 6). Due to the ligands' increased capacity to donate electrons as they bind with the tin metal, the complexes displayed more scavenging activity than the ligands [66]. The complexes displayed antioxidant activity in the order of: Ph_2SnL (**4**) > Bu_2SnL (**2**) Me_2SnL (**1**), > t-Bu_2SnL (**3**). The Phenyl complex (**4**) displayed highest activity, due to the phenyl ring's role in the donation of electron and also due to presence of the electron-donor group (ethoxy) in ortho position to the hydroxy group of the salicylaldehyde of ligand (H_2L), making it more effective antioxidant agents [43].

Table 6 Antioxidant activity using the DPPH method

Sample	IC_{50} (µg/mL)
1	69
2	61
3	89
4	47
Ascorbic acid	58

In-vitro Cytotoxic activity

The results of the MTT assay revealed that all of the organotin (IV) complexes showed cytotoxic activity against the breast cancer cells. When the cytotoxic potentials of the organotin (IV) complexes were compared, complex (**2**) exhibited the highest cytotoxic activity, with an IC_{50} value of 48.32± 0.04 µg/mL, followed by **(3)** > **(4)** > **(1)** > **(5)** > **(H_2L)** (Table 7). The butyl derivative showed the highest activity. Compared to ligands, diorganotin(IV) complexes (**1-5**) had higher levels of activity and the chelation theory can be used to explain these results. As ligands chelate to the metal centre, the metal's lipophilic character increases due to partial sharing of its positive charge with the donor R group and delocalization of the π electron that can occur in the entire chelate ring system. As a result, due to the complexes' increased lipophilicity, they can more readily pass-through cell membranes and bind with the DNA [43].

The higher activity of the dibutyltin(IV) complex (**2**), when compared to the diphenyl and dimethyl complexes, was consistent with previous findings, and can be explained by the optimal balance of cytotoxicity, solubility, and lipophilicity [44, 67-70]. But all the synthesized compounds were less active than cisplatin. The order of IC_{50} values was found to be in accordance with the order of K_b values, calculated from spectroscopic and electrochemical assay. So these results indicated that DNA-binding interaction studies can be used for determination of the anticancer potential of a drug.

Table 7 Inhibition action of ligand (**H_2L**) and complexes (**1-5**) to cancer cells *in vitro*

Sample code	IC_{50} µg/mL
H_2L	76.92± 0.03
1	55.49± 0.02
2	48.32± 0.04
3	51.49± 0.01
4	53.61± 0.02
5	55.59± 0.01
Cisplatin	5.94± 0.02

Conclusions

The Single Crystal X-ray study and spectroscopic data confirmed that the coordination of synthesized ligand with diorganotin(IV) moiety through ONO donor sites in a tridentate fashion, the oxygen atom of the hydroxy group of the hydrazide ligand (**H_2L**) that was engaged in the keto-enol tautomerization and the nitrogen atom of the azomethine group, producing a pentacoordinate geometry. The dimethyltin(IV) derivative (**1**) showed pentagonal-bipyramidal geometry around the Sn atom in solid state. UV-Vis spectroscopic, Cyclic voltammetric, and viscosity data for DNA binding studies of synthesized compounds suggested an intercalative as a mode of interaction, and the dibutyltin(IV) complex (**2**) showed the highest binding constant value. The negative values ΔG obtained in both UV-Vis spectroscopy, and CV indicated the spontaneity of complexes-DNA interactions. All the complexes were potential active antioxidants however complex (**4**) showed the highest DPPH antioxidant activity. These compounds also showed cytotoxicity against the human breast cancer line (MDA-MB-231). Therefore, the complex (**2**) may be a suitable candidate for the creation of novel medicine based on hydrazides. The outcomes of this series of organotin

complexes offer fresh optimism for the development of more effective antioxidant and anticancer compounds in the future.

Supplementary-Data:

Crystallographic data for the structure of complex (**1**) in this paper have been deposited with the Cambridge Crystallographic Data Centre, CCDC, 12 Union Road, Cambridge CB21EZ, UK. Copies of the data can be obtained free of charge on quoting the depository numbers CCDC-1906530 for **complex 1.** (Fax: +44-1223-336-033; E-Mail: deposit@ccdc.cam.ac.uk, http://www.ccdc.cam.ac.uk). The numbering scheme of ligand, organotin(IV) complexes, various spectra including IR, NMR UV and mass are provided as supporting material.

Acknowledgements

The author SR is thankful to Higher Education Commission of Pakistan for financial support. Under the PhD Indigenous Fellowship Scheme Phase-II, Batch-III, (PIN Code: 315-9545-2PS3-074) and HEC IRSIP (PIN Code: IRSIP 45 PSc 05).

Declaration of competing interest

Conflict of interest The authors declare that they have no known competing financial interests or personal relationships that could have appeared to influence the work reported in this paper.

References

[1] S. Dasari, P. Bernard Tchounwou, Eur. J. of Pharmacol. 740 (2014) 364-378.

[2] B. Rosenberg, L. Vancamp, J.E. Trosko, V.H. Mansour, Nature 222 (1969) 385-386.

[3] S. Dehghanpour, H.R. Pourzamani, M.M. Amin, K. Ebrahimpour, Aquat. Toxicol. (Amsterdam, Netherlands) 223 (2020) 105495.

[4] C.M. Allen, F. Lopes, R.T. Mitchell, N. Spears, Mol. Hum. Reprod. 26 (2020) 129-140.

[5] P. Zhao, M. Li, Y. Chen, C. He, X. Zhang, T. Fan, T. Yang, Y. Lu, R.J. Lee, X. Ma, J. Luo, G. Xiang, Int. J. Pharm. 570 (2019) 118638.

[6] T. Karasawa, P.S. Steyger, Toxicol. Lett. 237 (2015) 219-227.

[7] Y. Lin, H. Betts, S. Keller, K. Cariou, G. Gasser, Chem. Soc. Rev. 50 (2021) 10346-10402.

[8] Y. Li, B. Liu, H. Shi, Y. Wang, Q. Sun, Q. Zhang, Dalton Transactions 50 (2021) 14498-14512.

[9] A. Notaro, M. Jakubaszek, S. Koch, R. Rubbiani, O. Dömötör, É.A. Enyedy, M. Dotou, F. Bedioui, M. Tharaud, B. Goud, S. Ferrari, E. Alessio, G. Gasser, Eur. J. Chem. 26 (2020) 4997-5009.

[10] D. Rocco, L.K. Batchelor, G. Agonigi, S. Braccini, F. Chiellini, S. Schoch, T. Biver, T. Funaioli, S. Zacchini, L. Biancalana, M. Ruggeri, G. Pampaloni, P.J. Dyson, F. Marchetti, Eur. J. Chem. 25 (2019) 14801-14816.

[11] S. Saroya, S. Asija, N. Kumar, Y. Deswal, J. Devi, J. Indian Chem. Soc. 3 (2022) 100379.

[12] Nopitasari, T. Suhartati, Suharso, D. Herasari, K.D. Pandiangan, S. Hadi, J. Phys. Conf. Ser. 1 (2021) 012098.

[13] T. Anasamy, C.K. Thy, K.M. Lo, C.F. Chee, S.K. Yeap, B. Kamalidehghan, L.Y. Chung, Eur. J. Med. Chem. 125 (2017) 770-783.

[14] A. Attanzio, M. Ippolito, M.A. Girasolo, F. Saiano, A. Rotondo, S. Rubino, L. Mondello, M.L. Capobianco, P. Sabatino, L. Tesoriere, G. Casella, J. Inorg. Biochem. 188 (2018) 102-112.

[15] S.N. Syed Annuar, N.F. Kamaludin, N. Awang, K.M. Chan, Front. Chem. 9 (2021) 657599.

[16] S.K. Hadjikakou, Ozturk, II, M.N. Xanthopoulou, P.C. Zachariadis, S. Zartilas, S. Karkabounas, N. Hadjiliadis, J. Inorg. Biochem. 102 (2008) 1007-15.

[17] M.K. Amir, S. Khan, R. Zia ur, A. Shah, I.S. Butler, Inorganica Chim. Acta 423 (2014) 14-25.

[18] K.M. Lo, S.M. Lee, E.R.T. Tiekink, Zkrist-New Cryst St . 6 (2019) 1309-1311.

[19] M. Sirajuddin, S. Ali, Curr. Pharm. Des. 22 (2016) 6665-6681.

[20] S. Hadjikakou, N. Hadjiliadis, Coord. Chem. Rev. 253 (2009) 235-249.

[21] J. Devi, S. Pachwania, Phosphorus Sulfur Silicon Relat. Elem. 12 (2021) 1049-1060.

[22] M. Romero-Chávez, K. Pineda-Urbina, D. Pérez, F. Obledo, A. Flores-Parra, Z. Gomez-Sandoval, A. Organillo, J. Organomet. Chem. 862 (2018) 58-70.

[23] D. Kumar Dey, A. Lycka, S. Mitra, G.M. Rosair, J. Organomet. Chem. 689 (2004) 88-95.

[24] S.K. Hadjikakou, N. Hadjiliadis, Coord. Chem. Rev. 253(1) (2009) 235-249.

[25] M. Sirajuddin, S. Ali, A. Badshah, J. Photochem. Photobiol. B, Biol. 124 (2013) 1-19.

[26] Y. Zhou, Y. Li, Biophys. Chem. 107 (2004) 273-81.

[27] Y. Ni, D. Lin, S. Kokot, Talanta 65 (2005) 1295-302.

[28] M. Sirajuddin, A. Haider, N. Shah, A. Shah, M. Khan, Polyhedron 40 (2012) 19-31.

[29] P. Krishnamoorthy, P. Sathyadevi, A.H. Cowley, R.R. Butorac, N. Dharmaraj, Eur. J. Med. Chem. 46 (2011) 3376-87.

[30] W. Jiang, S. Fan, Q. Zhou, F. Zhang, D. Kuang, Y. Tan, Bioorg. Chem. 94 (2020) 103402.

[31] M. Yousefi, T. Sedaghat, J. Simpson, M. Shafiei, Appl. Organomet. Chem. 33 (2019) e5137.

[32] M. Mehmood, D. Imtiaz ud, M. Nawaz Tahir, I. Haq, S.S. Zahra, Inorganica Chim. Acta 486 (2019) 387-394.

[33] W.J. Jiang, Q. Zhou, M.Q. Liu, F.X. Zhang, D.-Z. Kuang, Y.X. Tan, Appl. Organomet. Chem. 33 (2019) e5092.

[34] M. Hong, H. Geng, M. Niu, F. Wang, D. Li, J. Liu, H. Yin, Eur. J. Med. Chem. 86 (2014) 550-561.

[35] W.L.F. Armarego, Purification of laboratory chemicals, Butterworth-Heinemann 2017.

[36] S. Shujah, S. Ali, N. Khalid, M.J. Alam, S. Ahmad, A. Meetsma, Chem. Pap. 72 (2018) 903-919.

[37] M. Tariq, N. Muhammad, M. Sirajuddin, S. Ali, N.A. Shah, N. Khalid, M.N. Tahir, M.R. Khan, J. Organomet. Chem. 723 (2013) 79-89.

[38] M. Sirajuddin, N. Uddin, S. Ali, M.N. Tahir, Spectrochim. Acta A Mol. 116 (2013) 111-121.

[39] M. Sirajuddin, V. McKee, M. Tariq, S. Ali, Eur. J. Med. Chem. 143 (2018) 1903-1918.

[40] A.N. M.A. Alaghaz, S.A.A. Aldulmani, Appl. Organomet. Chem. 33 (2019) e5135.

[41] A.A. Phadte, S. Banerjee, N.A. Mate, A. Banerjee, Biochem. Biophys. Rep. 18 (2019) 100629.

[42] N. Uddin, F. Rashid, S. Ali, S.A. Tirmizi, I. Ahmad, S. Zaib, M. Zubair, P.L. Diaconescu, M.N. Tahir, J. Iqbal, A. Haider, J. Biomol. Struct. Dyn. 38 (2020) 3246-3259.

[43] S. Saroya, S. Asija, N. Kumar, Y. Deswal, J. Indian Chem. Soc. 99 (2022) 100379.

[44] M. Yousefi, T. Sedaghat, J. Simpson, M. Shafiei, Appl. Organomet. Chem. 33 (2019) e5137.

[45] S. Shujha, A. Shah, N. Muhammad, S. Ali, R. Qureshi, N. Khalid, A. Meetsma, Eur. J. Med. Chem. 45 (2010) 2902-2911.

[46] T.P. Lockhart, W.F. Manders, J. Am. Chem. Soc. 109, (1987) 7015.

[47] S.M. Lee, H. Mohd. Ali, K.S. Sim, S.N. Abdul Malek, K.M. Lo, Inorganica Chimica Acta 406 (2013) 272-278.

[48] S. Shujah, N. Muhammad, A. Shah, S. Ali, N. Khalid, A. Meetsma, J. Organomet. Chem. 741 (2013) 59-66.

[49] W. Jiang, Y. Tan, Y. Peng, Int. J. Mol. Sci. 22 (2021) 13525.

[50] Z. Mandegani, Z. Asadi, M. Asadi, H.R. Karbalaei-Heidari, B. Rastegari, J. Chem. Soc., Dalton trans. 45 (2016) 6592-6611.

[51] T.R. Li, Z.Y. Yang, B.D. Wang, D.D. Qin, Eur. J. Med. Chem. 43 (2008) 1688-1695.

[52] X.L. Wang, H. Chao, H. Li, X.L. Hong, Y.J. Liu, L.F. Tan, L.N. Ji, J. Inorg. Biochem. 98 (2004) 1143-1150.

[53] S.N. Hakobyan, Proc. YSU B: Chem. Biol. Sci. 50 (2016) 51-54.

[54] M. Imran, T. Kondratyuk, F. Bélanger-Gariepy, Inorg. Chem. Commun. 103 (2019) 12-20.

[55] M. Sirajuddin, S. Ali, A. Haider, N.A. Shah, A. Shah, M.R. Khan, Polyhedron 40 (2012) 19-31.

[56] M. Tariq, R. Khan, A. Hussain, A. Batool, F. Rasool, M. Yar, K. Ayub, M. Sirajuddin, F. Ullah, S. Ali, J. of Coord. Chem. 74 (2021) 2407-2426.

[57] K. Liu, H. Yan, G. Chang, Z. Li, M. Niu, M. Hong, Inorganica Chim. Acta 464 (2017) 137-146.

[58] M. Shakeel, T.M. Butt, M. Zubair, H.M. Siddiqi, N.K. Janjua, Z. Akhter, A. Yaqub, S. Mahmood, Heliyon 6 (2020) e04124.

[59] N. Arshad, M.H. Bhatti, S.I. Farooqi, S. Saleem, B. Mirza, Arab. J. Chem. 9 (2016) 451-462.

[60] J.E.B. Randles, J. Chem. Soc. Faraday Trans. 44 (1948) 327-338.

[61] A. Ševčík, Collection of Czechoslovak, Chem. Commun. 13 (1948) 349-377.

[62] M. Shabbir, Z. Akhter, I. Ahmad, S. Ahmed, V. McKee, H. Ismail, B. Mirza, Polyhedron 124 (2017) 117-124.

[63] M. Aslanoglu, G. Ayne, Anal. Bioanal. Chem. 380 (2004) 658-663.

[64] J. Wang, Y. Li, C. Li, X. Zeng, T. Wenwei, X. Chen, Microchim. Acta 184 (2017) 1-8.

[65] H. Xu, X. Li, J. Zhang, Z. Zhang, K. Liu, Microchim. Acta 165 (2009) 415-420.

[66] A. Corona-Bustamante, J.M. Viveros-Paredes, A. Flores-Parra, A.L. Peraza-Campos, F.J. Martínez-Martínez, M.T. Sumaya-Martínez, Á. Ramos-Organillo, Molecules 15 (2010) 5445-5459.

[67] M. Khandani, T. Sedaghat, N. Erfani, M.R. Haghshenas, H.R. Khavasi, J. Mol. Struct. 1037 (2013) 136-143.

[68] B. Jousseaume, M. Pereyre, P.J. Smith, Blackie Academic & Professional, London, 1998.

[69] M. Hong, H. Geng, M. Niu, F. Wang, D. Li, J. Liu, H. Yin, Eur. J. Med. Chem. 86 (2014) 550-561.

[70] M. Hong, G. Chang, R. Li, M. Niu, New J. Chem. 40 (2016) 7889-7900.